

## Thermoluminescence kinetic in the case of a continuous distribution of trap centres over their activation energies

This article has been downloaded from IOPscience. Please scroll down to see the full text article.

1993 J. Phys.: Condens. Matter 5 7503

(<http://iopscience.iop.org/0953-8984/5/40/024>)

View [the table of contents for this issue](#), or go to the [journal homepage](#) for more

Download details:

IP Address: 171.66.16.96

The article was downloaded on 11/05/2010 at 01:58

Please note that [terms and conditions apply](#).

## Thermoluminescence kinetic in the case of a continuous distribution of trap centres over their activation energies

L N Kantorovich†||, A I Livshicz‡ and G M Fogel§

† Departamento de Química Física y Analítica, Universidad de Oviedo, 33006-Oviedo, Asturias, Spain

‡ Latvian Medical Academy, Dzirciema str.16, LV-1007, Riga, Latvia

§ Tel-Aviv University, Tel-Aviv, Israel

Received 26 February 1993, in final form 1 June 1993

**Abstract.** The integral equation method (IEM) proposed in our previous paper to describe the thermoluminescence (TL) kinetic in the general case of an arbitrary distribution of centres over their parameters in the framework of the band kinetic model is numerically implemented in this paper. The simplest model is considered, when the thermal ionization is inherent only in trap centres which are distributed over their activation energies because of a one-Gaussian-type curve. We study the form of the TL curves, dose dependences and some pre-heating computer experiments in order to distinguish between cases of really discrete and continuous distributions of centres. We have demonstrated that, in the case of large retrapping (in comparison with recombination), the application of the IEM appears to be quite important, and simple averaging of separate individual contributions of each centre leads to erroneous results.

### 1. Introduction

One of the most familiar approaches of studying the thermoluminescence (TL) processes in luminophors is based on the so-called band model. The TL process is described as a flow of electrons thermally released from trapping centres (TCs) through the lowest conduction band with their subsequent recombination on recombination centres (RCs) of a hole nature. This process is usually treated by solving a set of non-linear differential equations [1–4] for the electron concentration  $n_i^-(t)$  and hole concentrations  $n_j^+(t)$  occupying the  $i$ th and  $j$ th types of traps, respectively.

However, this method is relevant only if the microscopic interaction between different traps in the crystal is negligibly small (i.e. they are strongly separated from each other in the space) and therefore all traps can be regarded as almost independent. This means that all traps (i.e. defects) of the same chemical nature are associated really with one and the same type  $i$  of TC (or  $j$  of RC) with respect to the TL process in question. However, if the concentration of traps increases, the quantum interaction between them becomes significant and therefore defect bands within forbidden gaps appear to be wider. This means that the traps having the same chemical nature cannot be considered as traps of the same type from the viewpoint of the TL process, since they have different activation energies (measured downwards from the bottom of the conduction band).

The density  $\mathcal{N}(E)$  of states of the defect bands results in a continuous distribution  $\Psi(E) \propto \mathcal{N}(e)$  (normalized to unity) of traps over their activation energies  $E$ . Good evidence

|| Permanent address: Latvian Medical Academy, Dzirciema str.16, LV-1007, Riga, Latvia.

for the distribution of traps in quartz has been demonstrated recently [5]. Also, because of the broad TL peak observed for  $\text{Al}_2\text{O}_3:\text{C}$  thermoluminophor [6] there remains no doubt that it should be attributed to a wide continuous distribution over the trap activation energies. There are some other examples of continuous distributions of trap parameters (usually, over activation energies) available in the literature (see for instance the reviews in [4, 7]).

Of course, it is rather a complicated task to use the usual set of TL equations mentioned above to solve the kinetic problem of the continuous distribution of traps in practice. First, for every energy  $E_i$  which results in  $\mathfrak{N}(E_i) \neq 0$ , a new trap of the type  $i$  has to be associated. Thus, together with an infinite number of types  $i$  of traps we obtain an infinite number of TL equations.

Of course, the infinite set of equations can be simulated numerically by a large but finite set of them. However, it is not that easy and there are several reasons for this. Firstly, the number of equations needed to achieve convergency to the actual distribution is usually very large [5], resulting in considerable computational costs. Secondly, as our experience shows, systems of very many simultaneous differential equations exhibit many numerical problems (weakly controlled demands as to the precision along the numerical integration, instability problems, etc.) and, as the parameters of the model are chosen somewhat dramatically, the numerical scheme may diverge as well.

On the other hand, it is worth mentioning here that the usually treated case of a finite number of traps with discrete energy levels  $E_i$  (a discrete distribution) can also be treated using the notion of the continuous distribution

$$\Psi(E) \propto \sum_i \delta(E - E_i).$$

Moreover, from the practical point of view, a continuous distribution  $\Psi(E)$  containing, for example, a part  $\Psi'(E)$  which is too narrow (it has a quite small dispersion) can be considered physically as being compiled from a continuous part  $\Psi(E) - \Psi'(E)$  and the discrete level  $E_0$  (the mean value of the  $\Psi'(E)$ ). Thus, many cases faced in practice can be covered by a model in which the common continuous distribution  $\Psi(E)$  of traps is considered instead of the types  $i$  of them.

Usually [2, 8, 9] the case of a continuous distribution is treated by averaging the individual contributions  $J_E(t)$  produced by traps with different energies  $E$ , and the total output is assumed to be

$$J(t) = \int \Psi(E) J_E(t) dE. \quad (1)$$

In this approximation the retrapping is underestimated since only the retrapping to parent traps is allowed, while the retrapping to traps with other energies is completely forbidden. It is clear that this simple model works quite well only in the case of the first-order kinetic when the retrapping process is negligible compared with the recombination process. At the same time, the account of the 'interaction' of traps (in the sense of their retrapping) cannot be underestimated while considering the TL process in the course of the second-order kinetic [10]. However, in the latter case it is necessary to take into consideration the retrapping of carriers on every trap, i.e. we arrive at an infinite number of the TL equations, which turn out to be quite tedious and may be calculated in some simple cases only [5].

In our previous paper [11] we have developed a new approach, the integral equation method (IEM), which permits us to consider an arbitrarily complex TL process (within the same band model), including the case of a continuous distribution of hole and/or electron

traps over their various parameters (such as activation energies and frequency factors), in a physically transparent way. We have shown that the infinite set of the TL kinetic equations can be equivalently transformed into only two (although rather complicated) equations with respect to two new auxiliary functions  $z^-(t)$  and  $z^+(t)$ . They describe an accumulation of free charge carriers (electrons and holes) in the lowest conduction and highest valence bands, respectively, during the process of irradiation, temperature decay† and TL, which follow one after another.

The equations solved in the IEM represent the rigorous equivalent of the usual TL kinetic equations and therefore are equally applicable to the same class of physical problems. At the same time, they are formulated in such a way that can be used in the case of both discrete and continuous distributions. This means that in practice they are sufficiently more useful since they can be implemented for any problem whereas the usual approach based on the set of differential equations cannot. On first glance, however, the integral-differential equations of the IEM seem to be very complicated and, only for this reason, they may be completely useless. These arguments are also supported by the fact that the problem of the numerical solution of the equations of the IEM has not been discussed yet. That is why the goal of the present paper is to show the possibility of solving these equation numerically for a quite simple but physically interesting problem rather than considering some 'real' processes in some 'real' material and trying to reproduce some observations of a 'real' experiment. Our plan is to try to achieve the latter in subsequent papers.

In the next section we briefly give a description of the IEM and introduce a simple model used here. Some remarks concerning the numerical method implemented to solve the equations are made in the appendix. In section 3 the results of numerical calculations, including dose dependences for both a peak position and a peak intensity, will be given and discussed. The two physically interesting cases of small retrapping (SR) and large retrapping (LR) are compared. Also, we demonstrate the shapes of the TL curves for different Gaussian-type distributions  $\Psi(E)$  in order to compare the results obtained with those calculated for the case of a discrete distribution.

## 2. Basic model from the viewpoint of the integral equation method

In this paper we restrict ourselves to the following simple model. We suppose that only one discrete hole level is present and that the hole channel is used only during irradiation; it is also assumed that the hole thermal ionization is negligibly small (the corresponding thermal probability  $\omega^+ \simeq 0$ ). All equations are written in the case of a general continuous distribution  $\Psi(E)$  of the TCS over their activation energies  $E$ . However, actual calculations are done for the Gaussian-type form of the distribution  $\Psi(E)$ .

Since the general case of the IEM has been discussed in [11] (although quite formally), we shall consider here the detailed derivation of the IEM equations for the particular model used in the present paper. The general kinetic equations governing the processes within the framework of the band model under the assumptions made above are [1-3]

$$dn_E^-(t)/dt = N^- \sigma^- [v_E^- - n_E^-(t)] - \omega_E^- n_E^-(t) \quad (2a)$$

$$dn^+(t)/dt = N^+ \sigma^+ [1 - n^+(t)] - N^- A n^+(t) \quad (2b)$$

† A process which happens between the irradiation and the TL. It results in the additional redistribution of charge carriers due to the establishment of equilibrium after the abrupt end of irradiation.

$$dN^+(t)/dt = -N^+\sigma^+[1 - n^+(t)] + R \quad (2c)$$

$$N^- + \int n_E^-(t) dE = N^+ + n^+(t). \quad (2d)$$

The summation over the electronic traps in equation (2d) has been substituted by the integration over the energy  $E$ . The following notation has been adopted here:  $R$  is the generation rate of electron-hole pairs during the irradiation;  $\sigma^\pm$  are the trapping coefficients (it is assumed that  $\sigma^-$  does not depend on  $E$ );  $A$  is the recombination coefficient for electrons in the conduction band to interact with holes captured on the RC;  $\nu_E^- = \nu^- \Psi(E)$  is the concentration of the TCs with the energy  $E$ , distributed as a function  $\Psi(E)$ ,  $\nu^-$  being the total concentration of the TCs. Also the superscripts  $+$  and  $-$  are used to distinguish between the hole and electron components. Thus,  $N^+$  and  $N^-$  are the concentrations of free holes and electrons in the valence and the conduction bands, respectively, and  $n_E^-(t) dE$  and  $n^+(t)$  are the concentrations of the captured electrons and holes on the TCs (with the energy  $E$ ) and RC, respectively. Finally

$$\omega_E^-(t) = \omega_0 \exp(-E/kT)$$

is the probability of the thermal ionization of an electron from the TC with the energy  $E$ ,  $\omega_0$  being the appropriate frequency factor not depending on  $E$ , as is adopted here for simplicity;  $T$  is the absolute temperature, while  $k$  is Boltzmann's constant. All parameters are defined with respect to the RC concentration  $\nu^+$ , which can be chosen as a free parameter of the theory and has been set to unity.

Let us start with the irradiation process ( $R \neq 0$ ). We assume, as is usually done in such a study (see [5], for example) and is fulfilled in the experiment, that the corresponding temperature is constant and quite small and therefore the thermal ionization of electrons during the irradiation is negligible ( $\omega_E^- \simeq 0$ ). Thus, equation (2a) loses the last term on the right-hand side. Then, following the method developed in [11], we can solve formally the linear first-order differential equations (2a) and (2b) with reference to  $n_E^-(t)$  and  $n^+(t)$  and substitute the distributions obtained into equations (2c) and (2d). It was found in [11] that the auxiliary functions

$$z^\pm(t) = \int_0^t N^\pm(\tau) d\tau \quad z^\pm(0) = 0$$

are useful instead of the free-carrier concentrations  $N^\pm(t)$ . The new functions introduced describe the accumulation of the free charge in the bands during the processes.

On the assumption that the initial concentrations on the TC and RC are equal to zero at the beginning of the irradiation process, we have for the distribution of the concentrations

$$n_E^-(t) = \nu_E^- \{1 - \exp[-\sigma^- z^-(t)]\} = \nu^- \{1 - \exp[-\sigma^- z^-(t)]\} \Psi(E) \quad (3)$$

$$n^+(t) = \sigma^+ Q^+(t) \quad (4)$$

where

$$Q^+(t) = \int_0^t \frac{dz^+(\tau)}{d\tau} \exp[f^+(\tau) - f^+(t)] d\tau \quad (5a)$$

$$f^+(t) = \sigma^+ z^+(t) + Az^-(t). \quad (5b)$$

Then, the integration over  $E$  in equation (2d) can be performed quite easily since the only function of  $E$  is  $\nu_E^- \propto \Psi(E)$  (see equation (3)). Thus, we arrive at the following set of equations with respect to the new auxiliary functions in the case of the irradiation:

$$d^2 z^+(t)/dt^2 = R - \sigma^+ [1 - \sigma^+ Q^+(t)] dz^+(t)/dt \quad (6a)$$

$$dz^-(t)/dt + \nu^- \{1 - \exp[-\sigma^- z^-(t)]\} = dz^+(t)/dt + \sigma^+ Q^+(t). \quad (6b)$$

It is necessary to emphasize that equations (5) are exact for the model in question in the sense that they are a direct consequence of equations (2) of the usual band model kinetic. The concentrations of trapped carriers during the irradiation are obtained directly from the functions  $z^\pm(t)$  using equations (3) and (4).

The temperature decay process follows immediately after the irradiation and is defined by the condition  $R = 0$ . It can be described simply by the same set of equations (5) and (6) provided that both these processes are considered within the same time scale:  $0 \leq t \leq t_{\text{irr}}$  refers to the irradiation process,  $R \neq 0$ , while  $t > t_{\text{irr}}$  (up to infinity) refers to the temperature decay process,  $R = 0$ . The quantity  $t_{\text{irr}}$  is the irradiation time which directly affects the dose absorbed by the sample:  $D \propto R t_{\text{irr}}$ .

However, real calculations are carried out for a finite time interval while considering the temperature decay, since the physically correct condition describing the charge conservation law (see equations (2d), (3) and (4) in the limit  $t \rightarrow \infty$ )

$$n^+(\infty) = \int n_E^-(\infty) dE = \nu^- \{1 - \exp[-\sigma^- z^-(\infty)]\} \quad (7)$$

is achieved quite rapidly after stopping the irradiation.

While considering the TL process, it is more convenient to assume that both the processes considered above produce initial concentrations for it, and the time  $t$  is started again from  $t = 0$ . In this case we cannot neglect the last term on the right-hand side of equation (2a) describing the thermal release of electrons captured on the TCs. Nevertheless, equation (2a) can still be formally solved with respect to  $n_E^-(t)$ , giving [11]

$$n_E^-(t) = \{n_0 \exp[-f_E^-(t)] + \sigma^- \nu^- Q_E(t)\} \Psi(E) \quad (8)$$

where

$$Q_E(t) = \int_0^t \frac{dz^-(\tau)}{d\tau} \exp[f_E^-(\tau) - f_E^-(t)] d\tau \quad (9a)$$

$$f_E^-(t) = \sigma^- z^-(t) + \int_0^t \omega_E^-(\tau) d\tau \quad (9b)$$

where  $n_0 = n^+(\infty)$  represents the initial concentration established just after the end of temperature decay, see equation (7).

Then, during the TL process, the hole channel does not contribute (since  $R = 0$  and, at the initial time moment,  $N^+ = 0$ ), and therefore  $N^+ = 0$  at every time  $t > 0$ . Therefore, for this reason, the first term in the right-hand part of equation (2b) must be omitted whereas equation (2c) can be ignored. That is why equation (2b) can be easily solved, giving for the concentration of holes captured on the RC

$$n^+(t) = n_0 \exp[-Az^-(t)]. \quad (10)$$

Then, using equations (8) and (10), as well as the definition of the auxiliary function  $z^-(t)$ , we can rewrite equation (2d) in the following form:

$$\frac{dz^-(t)}{dt} + n_0[P(t) \exp(-\sigma^- z^-) - \exp(-Az^-)] = -v^- \sigma^- \int \Psi(E) Q_E^-(t) dE \quad (11)$$

where  $z^-(0) = 0$  and a new auxiliary function has been introduced:

$$P(t) = \int \Psi(E) \exp\left(-\int_0^t \omega_E^-(\tau) d\tau\right) dE. \quad (12)$$

Thus, in the IEM the TL process is governed by means of only one integral-differential equation (11), whereas two equations (6) (although considerably more simple) are needed as far as the irradiation and the temperature decay processes are concerned. The concentrations of localized charge carriers are calculated directly from the unique function  $z^-(t)$  using equations (8)–(10).

Finally, the TL intensity of the light emission (the TL output) is obtained in the usual way [1–3, 11] as the flux of recombination electrons (see equation (2b)):

$$J(t) \propto N^- An^+(t) = -dn^+(t)/dt \propto [dz^-(t)/dt] \exp[-Az^-(t)]. \quad (13)$$

Equation (10) has been used while deriving the last step in equation (13).

Thus, solving equations (9), (11) and (12) for only one unknown function  $z^-(t)$  it is possible to extract complete information about the TL process, including detailed dependences on the time of the concentrations of localized electrons and holes, equations (8) and (10), as well as the TL intensity, equation (13). Note that the TL current  $j_{TL}(t)$  can also be expressed through our auxiliary function  $z^-(t)$ , since

$$j_{TL}(t) \propto N^-(t) = dz^-(t)/dt.$$

However, we have not calculated the current in this paper.

Both sets of equations, equations (5) and (6) and equations (9), (11) and (12) are solved numerically by means of an indirect finite-difference method. Some details of the schemes developed for that purpose can be found in the appendix.

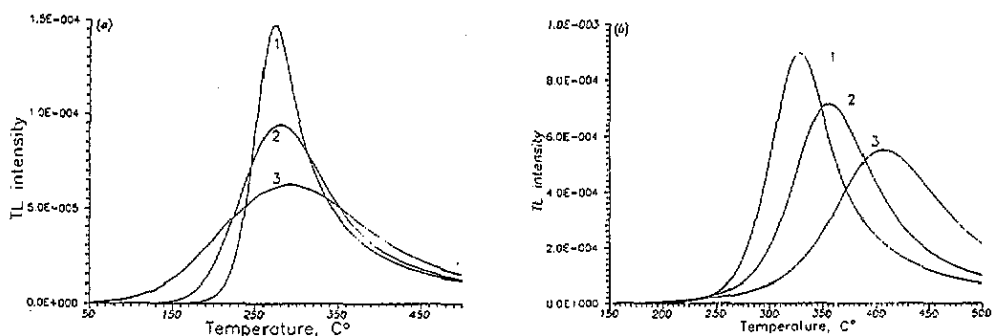
### 3. Results and discussion

In order to investigate the general properties of the equations stated above we have considered a model in which  $\Psi(E)$  is represented as one Gaussian with the mean value of the trap energy  $E_0 = 1.5$  eV and dispersions ranging from  $d_0 = 0.01$  up to  $d_0 = 0.2$ . The retrapping coefficient was chosen as follows:  $\eta = \sigma^-/A = 10^{-2}$  (SR or the first-order kinetic case),  $\eta = 1$  (an intermediate kinetic) and  $\eta = 10^2$  (LR or the case of the second-order kinetic). All other parameters used in the calculations are listed in table 1. All calculations discussed below are carried out by means of the consequent scheme; for each set of parameters we performed all three stages (irradiation, temperature decay and TL) one after another using the output of the current stage as the input for the subsequent stage.

In figure 1 we have represented TL curves calculated by means of our rigorous equations in the case of a small dose (the irradiation time  $t_{ir} = 0.1$  s) for different retrapping probabilities and different shapes of the Gaussian, starting from the narrowest ( $d_0 = 0.01$ ,

**Table 1.** Parameters used in the present calculations (first four parameters are given relatively to the  $\nu^+$ ).

Parameter	Value
$\nu^-$	1.0
$A$	1.0
$\sigma^+$	1.0
$R$	1.0
$E_0$	1.5 eV
$\omega_0$	$10^{13} \text{ s}^{-1}$
Heating rate	$1 \text{ K s}^{-1}$
Step over time	0.5 s
Step over energy	$d_0/4$

**Figure 1.** TL curves calculated numerically for the cases of small retrapping, (a)  $\sigma^-/A = 10^{-2}$  and large retrapping, (b)  $\sigma^-/A = 10^2$ . Curve 1:  $d_0 = 0.01$ ; curve 2:  $d_0 = 0.1$ ; curve 3:  $d_0 = 0.2$ .

almost the case of the discrete level with  $E = E_0$  and  $\nu = \nu^-$ ), and ending with a rather spread distribution ( $d_0 = 0.2$ ). It is seen that, the larger the dispersion  $d_0$ , the wider is the corresponding TL curve, as it should be. Then, it is also evident from figure 1(a) that in the case of SR ( $\eta = 10^{-2}$ ) we observe TL curves which have almost equal decreasing parts and almost unchanged peak positions with respect to the Gaussian chosen. The opposite situation is observed in the case of LR (figure 1(b)); we see a definite shift towards high temperatures of the peak positions ( $T_{\max}$ ) with increasing  $d_0$ .

This behaviour is explained not only by peculiarities of the second-order kinetic which occur here (non-linear dependence of the TL intensity on the initial concentration of localized carriers [1, 12]) but also by the complex retrapping which is fully taken into account in the IEM. In fact, released electrons have an opportunity to be retrapped on deeper TCs and in this way to increase their population [5, 10]. This leads to a definite increase in the deepest TC weights in the TL curve (the concentrations  $n_E^-(t)$  are no longer proportional to  $\Psi(E)$ ; see equation (8)) and results in a total shift in the TL curve in the direction of high temperatures. Note that this fact is ignored in the approximate schemes mentioned in the introduction, when all traps are considered as independent. Moreover, it is clear that this shift cannot be obtained in principle by means of that simple method.

The same curves are shown in figure 2 but in a different way; in both figure 2(a) and figure 2(b) we have fixed  $d_0$  and varied only the ratio  $\eta = \sigma^-/A$ . The shift in the TL curves with increasing ratio  $\eta$  is also evident here. Note that, in spite of the same irradiation time



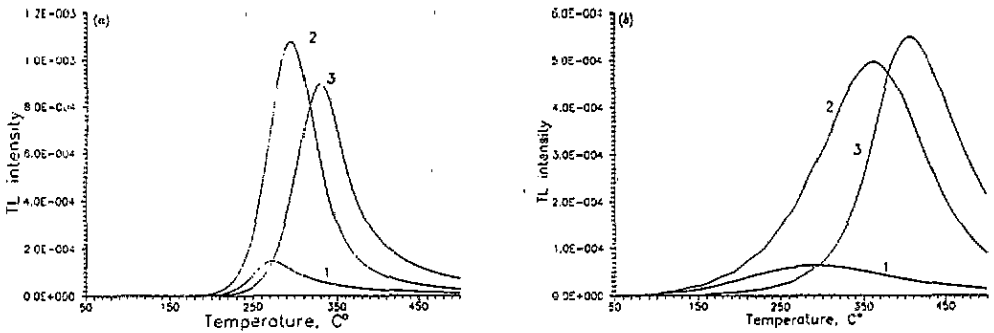


Figure 2. TL curves calculated numerically for the cases of a discrete distribution, (a)  $d_0 = 0.01$ , and a continuous distribution, (b)  $d_0 = 0.2$ . Curve 1:  $\sigma^-/A = 10^{-2}$ ; curve 2:  $\sigma^-/A = 1$ ; curve 3:  $\sigma^-/A = 10^2$ .

$t_{\text{irr}}$ , the real dose absorbed by the sample is different for various  $\eta$ -values since different retrapping conditions lead to different populations of traps during the irradiation process. That is why areas under each curve in figure 2 are different and increase together with the increase in the role played by the retrapping. It is seen also that the relative intensity of peaks shown in figure 2 changes from the case  $d_0 = 0.01$  (figure 2(a)) to  $d_0 = 0.2$  (figure 2(b)) which also demonstrates the important role of the retrapping.

The TL peak intensities  $J_{\text{max}}$  at the maximum as well as the peak positions  $T_{\text{max}}$  are represented for some dose interval ( $10^{-3}$  s  $<$   $t_{\text{irr}}$   $<$   $10^4$  s) in figures 3(a) and 3(b), respectively. We see from figure 3(a) that the TL intensity saturates for larger doses as  $\eta$  decreases. This property is apparently valid because the recombination process occurs during the irradiation and the temperature decay; in the case of SR a larger dose is needed to achieve saturation (when all traps are completely full; compare [5]) than in the case of LR. In order to explain the other peculiarities of the curves in figure 3 we have to address the detailed physical picture.

Let us consider first the case of the narrow distribution ( $d_0 = 0.01$ ; broken curves). As the retrapping factor  $\eta$  increases, the TL peak shifts to higher temperatures,  $T_{\text{max}}(\text{LR}) > T_{\text{max}}(\text{SR})$ , owing to delay in the release of electrons from the traps (figure 3(b)). However, this effect is suppressed for large doses, and  $T_{\text{max}}$  tends to smaller values (for given  $\eta$ ), since at the beginning of the TL process all traps are almost full, and the retrapping almost does not contribute. As a result, more electrons have a possibility of being released earlier from their traps during the heating. At the same time the TL peaks are broader for the LR than for the SR case (figure 3(a)), since in the former case it is more difficult to release electrons from their traps. Nevertheless, the inequality  $J_{\text{max}}(\text{LR}) < J_{\text{max}}(\text{SR})$  is valid only under comparatively large doses, when in both cases (LR and SR) we have completely full traps and  $n_0(\text{LR}) = n_0(\text{SR})$ . For smaller doses, however, another effect dominates, connected with the charge accumulation during the irradiation. Therefore we have here  $n_0(\text{LR}) > n_0(\text{SR})$ , and consequently  $J_{\text{max}}(\text{LR}) > J_{\text{max}}(\text{SR})$  (figure 3(a)).

The same analysis also holds for the case of a wide continuous distribution ( $d_0 = 0.2$ ; full curves). Let us compare this case with the previous one. Evident differences are explained by the role of a number of new factors which become important as  $d_0$  increases. Indeed, instead of almost one trap level  $E = E_0$  as in the former case, we deal here with a comparatively wide distribution of trap levels in the forbidden gap, although the total concentration of coupled electrons (and holes) is the same for given  $\eta$ . It apparently leads

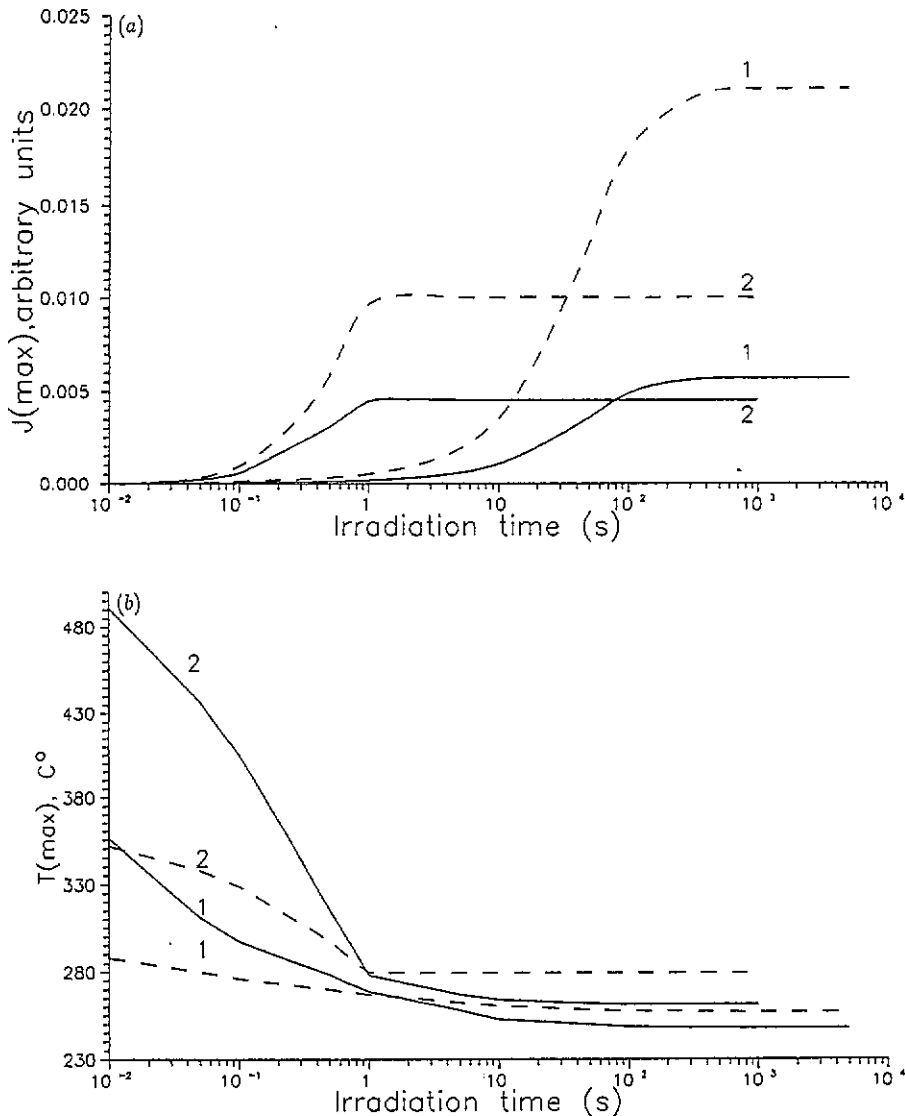


**Figure 3.** The dependence of (a) the  $\pi$  peak intensity and (b) the position in the maximum, on the irradiation time for the case of small retrapping, curve 1,  $\sigma^-/A = 10^{-2}$ ; and large retrapping, curve 2,  $\sigma^-/A = 10^2$ , full curve  $d_0 = 0.2$ ; broken curve  $d_0 = 0.01$ .

to broadening of the TL peak ( $\eta$  is fixed) and to a decrease in its intensity at the maximum. That is why all the full curves in figure 3(a) appear to be below the corresponding broken curves.

Then, especially in the case of LR, the retrapping on deeper levels also plays a significant role. For small doses when the traps are far from full, the retrapping results in a pronounced redistribution of trapped electrons, resettling them from shallow levels (located at the left-hand edge of the Gaussian) to deep levels (located at the right-hand edge of the Gaussian), and leads to larger  $T_{\max}$ -values. This effect becomes more important as  $\eta$  increases. That is why in figure 3(b) for small doses ( $t_{\text{irr}} < 1 \text{ s}^{-1}$ ) we observe all the full curves lying above the broken curves (for the same  $\eta$ ), and at the same time the difference

$\Delta T(\text{LR}) = T_{\text{max}}(\text{LR}, d_0 = 0.2) - T_{\text{max}}(\text{LR}, d_0 = 0.01)$  is larger than  $\Delta T(\text{SR})$  calculated in the same way for SR. In the region of large doses ( $t_{\text{irr}} > 1 \text{ s}^{-1}$ ) and for LR, all traps are completely full after the temperature decay process. Therefore, the effect of retrapping is almost switched off, and for the wide distribution (full curves) we observe an even smaller  $T_{\text{max}}$  than for the narrow distribution (broken curves) in the region of large doses (figure 3(b)). Of course, this difference decreases as  $\eta$  decreases.

Note that the crossing of the full and broken curves for SR (see figure 3(b)) occurs at almost the same dose value ( $t_{\text{irr}} \approx 1 \text{ s}^{-1}$ ) as for LR. The main explanation of this originates from the fact that the total retrapping probability is defined as the product of the retrapping coefficient  $\sigma^-$  and the number  $\nu_E^- - n_E(t)$  of free places on the traps. For large  $\eta$  values (LR) the retrapping is suppressed only just before and within the saturation region, whereas for small  $\eta$  values (SR) this effect starts substantially before the saturation region, since  $\sigma^-(\text{SR})/\sigma^-(\text{LR}) = 10^{-4}$  in our calculations.

Thus we see that figure 3 cannot be correctly explained without addressing the retrapping to deeper levels. This effect is completely taken into account in our equations of the IEM, while it is ignored in all the usual approaches based on the assumption of independent trap levels (see equation (1)). Note that the effect of the retrapping has also been correctly considered in [5]; however, the direct numerical integration of the initial set of the kinetic equations (2) was implemented there (they had to consider 96 energy points  $E_i$ , and therefore 96 equations (2a) were explicitly considered in order to achieve good convergency to the actual distribution of traps).

The last example regarded in the present paper deals with the following computer experiment: let a sample be subjected to some irradiation dose  $D \propto t_{\text{irr}}$ . Then, we heat the sample linearly up to some temperature  $T_{\text{preh}}$ , immediately cool it to room temperature and heat it again (at the same rate) until all localized electrons are released. In this way we obtain two TL peaks, shifted with respect to each other. This computer experiment has been repeated for different  $T_{\text{preh}}$ .

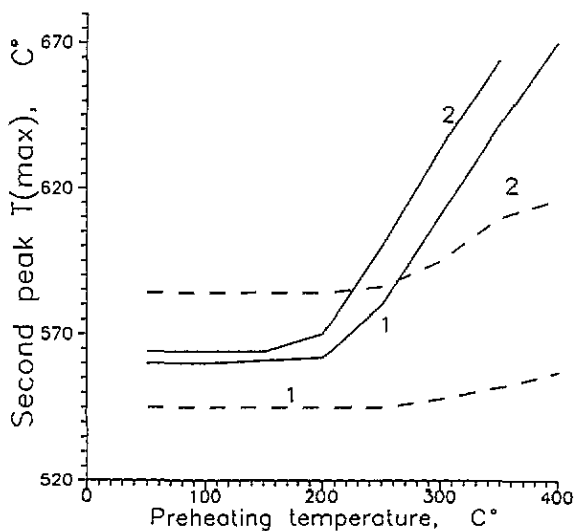


Figure 4. The second peak position  $T_{\text{max}}$  versus the preheating temperature  $T_{\text{preh}}$  from the computer experiment explained in the text: curve 1:  $\sigma^-/A = 10^{-2}$ ; curve 2:  $\sigma^-/A = 10^2$ . Full curve  $d_0 = 0.2$ ; broken curve  $d_0 = 0.01$ .

The dependence of the second peak position  $T_{\text{max}}$  on the pre-heating temperature  $T_{\text{preh}}$  is shown in figure 4. It is seen that in the case of the first-order kinetic and the discrete distribution ( $d_0 = 0.01$ ) the peak positions remain almost unchanged under the  $T_{\text{preh}}$

variation. However, on increasing  $d_0$  (i.e. the role of retrapping in deeper traps) a significant shift in the second peak is observed as  $T_{\text{preh}}$  is increased. Note also that this shift occurs even for the 'discrete' distribution ( $d_0 = 0.01$ ) in the case of the second-order kinetic ( $\eta = 10^2$ ), but this effect becomes substantially more important for a large continuous distribution width (i.e. large  $d_0$ ).

Evidently, this behaviour is due to the complex character of the traps in question. Indeed, during the first (pre-heating) step (heating to  $T_{\text{preh}}$ ), only the TCs which are active at those temperatures are released. This results in some alternation of the initial distribution of electrons from  $n_E^-(t) \propto \Psi(E)$  (at the beginning of the first step; see equation (3)) to that given by equation (8) (after the first step and at the beginning of the second step). Thus, deeper TCs become more important in the second step and produce a shift in the TL peak in the high-temperature direction. We think that the same experiment but performed in a laboratory may indicate the existence of the continuous distribution of traps in a sample.

#### 4. Conclusions

In the present paper we have demonstrated some results of the TL simulation in the model in which TCs are considered as continuously distributed over their activation energies. We have shown that the new equations of the IEM derived in [11] for the first time may be effectively numerically solved, leading to a time-efficient and stable numerical scheme. The results obtained demonstrate quite evidently their correct physical meaning, confirming the validity of the solutions. We hope that the IEM can be implemented in a wide range of problems of solid state TL dosimetry.

#### Acknowledgments

One of the authors (LK) is grateful to the Direccion General de Investigacion Cientifica y Technica (Spain) for grant SAB92-0226, which allowed us to finish this work.

#### Appendix

In the method developed in the present paper the usual net of times is introduced:  $t_i = i \Delta t$  ( $i = 0, 1, 2, \dots$ ). All the derivatives are substituted by finite differences using the function values at the current ( $i$ ) and at the preceding ( $i - 1$ ) time moments. For instance,  $dz^-(t_i)/dt \sim dz_i^-/dt = (z_i^- - z_{i-1}^-)/\Delta t$ . However, several important points ought to be mentioned here.

(i) In the case of equations (5) and (6) we have found it convenient to split the set of second-order equations into a set of first-order equations by making use of the substitution  $y(t) = z^+(t)$ .

(ii) The integrals  $Q^+(t)$  (equation (5a)) and  $Q_E(t)$  (equation (9a)) are calculated by means of the trapezoidal method and are considered at the preceding time moment.

(iii) The integrals over the energy  $E$  in equations (11) and (12) were calculated by means of the well known Simpson rule on a net  $\{E_j\}$  of energy points.

(iv) It was found to be quite important, however, to take into account correctly the non-linear character (over the unknown function  $z^-(t)$ ) of the exponents on the left-hand sides of equations (6b) and (11). This means that these exponents were considered at the current

time moment  $t_i$  and the corresponding non-linear algebraic equations over  $z_i^-$  were solved at each iteration (for each point  $t_i$ ) in both cases under consideration. Note that, in the direct finite-difference methods, only the derivatives involve the function at the current time moment whereas the residual part of the equations are considered at the preceding time moment. Our analysis showed, however, that this simple method fails for the problems under consideration.

The numerical calculating schemes developed in this way were checked very carefully using different heating regimes including very complicated regimes (for instance, a staircase with different steps used in the fractional glow-curve experiments [2, 9]). They were found to be quite stable and cheap and demand very small time or energy discretization intervals ( $\Delta t$  and  $\Delta E$ , respectively).

## References

- [1] Antonov-Romanovski V V 1966 *Kinetic Photoluminescence of Crystal Phosphors* (Moscow: Nauka) (in Russian)
- [2] Zakis Ju, Kantorovich L, Kotomin E, Kuzovkov V, Tale I and Shluger A 1991 *Models of Processes in Wide-Gap Crystals with Defects* (Riga: Zinatne) (in Russian)
- [3] Horowitz Y S 1984 *Thermoluminescence and Thermoluminescent Dosimetry* vol 3 (Boca Raton, FL: Chemical Rubber Company)
- [4] Chen R and Kirsh Y 1981 *Analysis of Thermally Stimulated Processes* (Oxford: Pergamon)
- [5] Hornyak W F, Chen R and Franklin A 1992 *Phys. Rev. B* **46** 8036
- [6] Gotlib V I, Akselrod M S, Kortov V S and Kravetsky D 1990 *Radiat. Prot. Dosim.* **32** 15
- [7] McKeever S W S 1984 *Radiat. Prot. Dosim.* **8** 81; 1985 *Thermoluminescence of Solids* (Cambridge: Cambridge University Press)
- [8] Hagekyriakov J and Fleming R J 1982 *J. Phys. D: Appl. Phys.* **15** 163
- [9] Tale I 1981 *Izv. Akad. Nauk. SSSR, Ser. Fiz.* **15** 245
- [10] Bull R K, McKeever S W S, Chen R, Mathur V K, Rhodes J and Brown M D 1986 *J. Phys. D: Appl. Phys.* **19** 1321; Bull R K 1986 *Radiat. Prot. Dosim.* **17** 459
- [11] Kantorovich L N, Fogel G M and Gotlib V I 1990 *J. Phys. D: Appl. Phys.* **23** 1219
- [12] Luschnik Ch B 1955 *Trap Centers Investigations in Alkali Halide Crystallophosphors* (Tartu: Trudij IPA Akademii Nauk Estonskoi SSR) (in Russian)